Electrochemical synthesis of ammonia from wet nitrogen via a dual-chamber reactor using La0.6Sr0.4Co0.2Fe0.8O3−δ-Ce0.8Gd0.18Ca0.02O2−δ composite cathode

Amar, IA, Lan, R, Humphreys, J & Tao, S

Original citation:
Amar, IA, Lan, R, Humphreys, J & Tao, S 2017, 'Electrochemical synthesis of ammonia from wet nitrogen via a dual-chamber reactor using La0.6Sr0.4Co0.2Fe0.8O3−δ-Ce0.8Gd0.18Ca0.02O2−δ composite cathode' *Catalysis Today*, vol 286, pp. 51-56
https://dx.doi.org/10.1016/j.cattod.2016.09.006

DOI 10.1016/j.cattod.2016.09.006
ISSN 0920-5861

Publisher: Elsevier

Catalysis Today 286 (2017) 51–56

Contents lists available at ScienceDirect

Catalysis Today

journal homepage: www.elsevier.com/locate/cattod

Electrochemical synthesis of ammonia from wet nitrogen via a dual-chamber reactor using $La_{0.6}Sr_{0.4}Co_{0.2}Fe_{0.8}O_{3-\delta}$-$Ce_{0.8}Gd_{0.18}Ca_{0.02}O_{2-\delta}$ composite cathode

Ibrahim A. Amar [b], Rong Lan [a], John Humphreys [a], Shanwen Tao [a,c,*]

[a] School of Engineering, University of Warwick, Coventry CV4 7AL, UK
[b] Department of Chemistry, Faculty of Sciences, Sebha University, Sebha, Libya
[c] Department of Chemical Engineering, Monash University, Clayton, Victoria 3800, Australia

ARTICLE INFO

Article history:
Received 17 May 2016
Received in revised form 29 July 2016
Accepted 9 September 2016
Available online 17 September 2016

Keywords:
Electrochemical synthesis
Ammonia
Oxygen vacancy
Oxide-carbonate composite electrolyte
$La_{0.6}Sr_{0.4}Co_{0.2}Fe_{0.8}O_{3-\delta}$

ABSTRACT

A $La_{0.6}Sr_{0.4}Co_{0.2}Fe_{0.8}O_{3-\delta}$-$Ce_{0.8}Gd_{0.18}Ca_{0.02}O_{2-\delta}$ composite cathode was used to investigate the electrochemical synthesis of ammonia from wet nitrogen. Wet nitrogen was flown through a dual chamber reactor under atmospheric pressure leading to the successful synthesis of ammonia. Ammonia was synthesised at a rate of 1.5×10^{-10} mol s^{-1} cm^{-2} at 400 °C when applying a dc voltage of 1.4 V, which is the highest reported to date. This rate is twice that of the observed ammonia formation rate (7×10^{-11} mol s^{-1} cm^{-2}) when Co-free cathode, $La_{0.6}Sr_{0.4}FeO_{3-\delta}$-$Ce_{0.8}Gd_{0.18}Ca_{0.02}O_{2-\delta}$ was used as the cathode catalyst. A higher catalytic activity for ammonia synthesis may be obtained when using a catalyst with high oxygen vacancies, with the introduction of oxygen vacancies at the cathode being a good strategy to improve the catalytic activity of ammonia synthesis.

1. Introduction

With a global production of around 150 million tons produced annually, ammonia is the second most produced inorganic chemical in the world [1–3]. The conventional Haber-Bosch process for ammonia synthesis uses fossil fuels such as natural gas or coal as its energy sources which lead to the release of about 300 million tons of CO_2 per year [4]. To reduce CO_2 from the ammonia industry, it is desired to replace the current energy sources with low carbon renewable resources such as renewable electricity. However, the development of energy storage for renewable electricity is still an urgent challenge. This is due to the nature of intermittence of energy sources such as wind and solar making it difficult to predict when they will be available. In Germany, for a certain period of time, the integration of large scale renewable electricity from solar and wind cause a negative electricity price [5]. In the UK, because they produced more electricity than the UK Grid could handle, wind farms were paid £30 million in 2013 and £53 million in 2014 to stand idle [6]. These problems remain unresolved and turbines have to be shut down at certain periods of time because the produced power is too much for Britain's electricity network to cope with. With the integration of low carbon renewable electricity, energy storage is becoming an urgent challenge. In various energy storage technologies, pumped hydro has proven to be the most useful, however, its implementation is limited due to restrictions imposed by location and available capacity. New technologies such as battery, flow battery, supercapacitor, flying wheel, compressed air etc. have also been investigated for energy storage, however; none of these new technologies can meet the requirements on cost and durability. Hydrogen production from the electrolysis of water has been demonstrated in Germany to adsorb the 'extra' electricity but it is still quite expensive. While the existing global market and infrastructure are already in place it has been proposed that it may be more viable to produce ammonia instead of hydrogen [7]. The electrochemical synthesis of ammonia using renewable electricity is one of the promising alternatives which will alleviate the pressure on renewable energy storage while also generating a new ammonia industry with a low carbon footprint [8–19]. It has been reported that if the cost for renewable electricity is not high then the cost from the electrochemical synthesis of ammonia will be comparable to that of the existing methods [20]. This technology will prove to be very attractive if we consider the negative price for renewable electricity. In early studies, H_2 and N_2 were normally used as the precursors in the electrochemical synthesis of ammonia. In

* Corresponding author at: University of Warwick, School of Engineering, Coventry CV4 7AL, UK.
E-mail address: S.Tao.1@warwick.ac.uk (S. Tao).

http://dx.doi.org/10.1016/j.cattod.2016.09.006

2009, for the first time, Skodra and Stoukides studied electrochemical synthesis of ammonia from steam (H_2O) and N_2. They achieved this using a ceramic electrolytic cell based on either a proton (H^+) or oxygen ion (O^{2-}) conducting oxide electrolyte with a Ru/MgO catalyst as the working electrode (cathode), by using steam as the hydrogen source they thereby successfully eliminated the hydrogen production stage [21]. This will provide a more efficient process for ammonia production with a few papers already published on using steam and N_2 to electrochemically synthesise ammonia based on an oxide cathode [13,22,23]. In a previous report, we found that $La_{0.6}Sr_{0.4}FeO_{3-\delta}$-$Ce_{0.8}Gd_{0.18}Ca_{0.02}O_{2-\delta}$ composite is a reasonably good cathode catalyst for electrochemical synthesis of ammonia from wet N_2 with a maximum rate of ammonia formation of 7×10^{-11} mol s^{-1} cm^{-2} observed at a temperature of 400 °C when the applied voltage was 1.4 V [24]. On the other hand, it has been recognised that oxygen vacancies may play a key role in achieving a high catalytic activity for ammonia synthesis. It has been reported that surface hydroxyl radicals, which were formed on reduced CeO_2 through the reaction between steam and oxygen vacancies in Co/CeO_2 ammonia synthesis catalyst, could enhanced the catalytic activity [25]. This increase in activity was explained through the dissociation of hydrogen atoms on the Co surface reacting with hydroxyl species on the CeO_2 surface forming water, thereby leaving the Co surface for the competing reaction, the dissociation of nitrogen to nitrogen atoms which is the rate-determining step [25]. When using perovskite oxide cathodes accompanying with oxygen vacancies in the lattice for electrochemical synthesis of ammonia from wet N_2, the oxygen vacancies in oxide cathode will react with H_2O to form charged protons according to the following reaction [26],

$$V_O^{\bullet\bullet} + H_2O + O_O^{\times} \Rightarrow 2OH_O^{\bullet} \quad (1)$$

Due to their positive charge the formed proton defects $OH_O^{\bullet}$ will be more prone to receiving electrons than neutron H_2O. In the presence of N_2, these defects may further react with N_2 to form NH_3 at the cathode,

$$6OH_O^{\bullet} + N_2 + 6e^- \Rightarrow 2NH_3 + 6O_O^{\times} \quad (2)$$

Therefore oxygen vacancies can be potential reaction sites at the cathode. Combining reactions (1) and (2), the reaction at the cathode is:

$$N_2 + 3H_2O + 3V_O^{\bullet\bullet} + 6e^- \Rightarrow 2NH_3 + 3O_O^{\times} \quad (3)$$

At the anode, O_2 is formed through lattice oxygen losing electrons according to the following reaction,

$$3O_O^{\times} \Rightarrow 3/2O_2 + 3V_O^{\bullet\bullet} + 6e^- \quad (4)$$

The formed oxygen vacancies $V_O^{\bullet\bullet}$ will transfer to the cathode to further react with H_2O forming proton defects according to reaction (1).

Combining reactions (3) and (4), the overall reaction is:

$$N_2 + 3H_2O \Rightarrow 2NH_3 + 3/2O_2 \quad (5)$$

From the analysis above, it can be seen that oxygen vacancies may play an important role in the electrochemical synthesis of ammonia, this is due to the formation of charged proton defects $OH_O^{\bullet}$ as intermediates according to reaction (1). From this point of view, the presence of oxygen vacancies at the cathode may facilitate the enhanced catalytic activity of ammonia synthesis.

Although there are a significant amount of oxygen vacancies in $La_{0.6}Sr_{0.4}FeO_{3-\delta}$, the partial replacement of Fe at the B-site by Co forming $La_{0.6}Sr_{0.4}Fe_{1-x}Co_xO_{3-\delta}$ has been reported to significantly increase of the concentration oxygen vacancies with a larger δ in LSCF [27]. In the $La_{0.6}Sr_{0.4}FeO_{3-\delta}$ series, $La_{0.6}Sr_{0.4}Co_{0.2}Fe_{0.8}O_{3-\delta}$ (LSCF) has been widely studied as a cathode for solid oxide fuel cells and membrane materials used for oxygen separation [28–30]. Therefore a higher catalytic activity is expected to be exhibited by LSCF than that of the Co-free perovskite oxide $La_{0.6}Sr_{0.4}FeO_{3-\delta}$.

The transfer of oxygen vacancies from the anode to the cathode surface to complete the cathode reaction may also be facilitated by the oxygen vacancies in doped CeO_2 such as $Ce_{0.8}Gd_{0.18}Ca_{0.02}O_{2-\delta}$ [31]. In this paper, results for the electrochemical synthesise of ammonia using wet nitrogen in via a dual-chamber reactor using $La_{0.6}Sr_{0.4}Co_{0.2}Fe_{0.8}O_{3-\delta}$-$Ce_{0.8}Gd_{0.18}Ca_{0.02}O_{2-\delta}$ composite cathode are presented. The catalytic activity of $La_{0.6}Sr_{0.4}Co_{0.2}Fe_{0.8}O_{3-\delta}$ was found to be higher than that of Co-free analogue $La_{0.6}Sr_{0.4}FeO_{3-\delta}$.

2. Experimental

2.1. Materials synthesis

A combined EDTA-citrate complexing sol-gel process was used to synthesise the $La_{0.6}Sr_{0.4}Co_{0.2}Fe_{0.8}O_{3-\delta}$ (LSCF) catalyst. Lanthanum oxide (La_2O_3, Alfa Aesar, 99%), strontium nitrate ($Sr(NO_3)_2$, Alfa Aesar, 99%), cobalt nitrate ($Co(NO_3)_2{\cdot}6H_2O$, Sigma Aldrich, 98+%) and iron nitrate nonahydrate ($Fe(NO_3)_3{\cdot}9H_2O$, Alfa Aesar, 98%) were used as starting materials. To remove the absorbed water La_2O_3 was first dried at 700 °C for 2 h. A lanthanum nitrate aqueous solution was then formed by dissolving La_2O_3 in diluted nitric acid. Calculated amounts of $Sr(NO_3)_2$, $Co(NO_3)_2{\cdot}6H_2O$ and $Fe(NO_3)_3{\cdot}9H_2O$ were dissolved in deionised water before being added to the lanthanum nitrate solution. Citric acid and ethylenediaminetetraacetic acid (EDTA), with a molar ratio of citric acid: EDTA: metal cations of 1.5:1:1 were then added as complexing agents. The pH value was then adjusted to around 6 through the addition of dilute aqueous ammonia solution to the mixed solution. a black sticky gel was then obtained by evaporating this solution on a hot plate. The as-prepared gel was pre-fired and then transferred to an alumina crucible and calcined in air at 900 °C for 2 h with heating/cooling rates of 5 °C min^{-1} to obtain single phase LSCF.

$Sm_{0.5}Sr_{0.5}CoO_{3-\delta}$ (SSCo) has been previously reported as an excellent cathode for intermediate temperature SOFCs [32]. Therefore in the ammonia electrochemical synthesis cell used in this study, SSCo was used as the anode. The activity of the oxygen evolution reaction at the anode was further increased by combining SSCo with an O^{2-} ionic conductor, ceria co-doped with Ca and Gd $Ce_{0.8}Gd_{0.18}Ca_{0.02}O_{2-\delta}$ (CGDC) powders, to form a composite anode. CGDC was also synthesised via the previously described combined citrate-EDTA complexing sol-gel process [24]. In order to prepare the composite electrolyte, CGDC was mixed in a weight ratio of 70:30 with the ternary carbonate ($(Li/Na/K)_2CO_3$) as previously described [22]. In order to improve the transfer of oxygen ions in the form of oxygen vacancies and thereby improve the ammonia synthesis activity, CGDC was also integrated to the cathode to form a composite cathode.

2.2. Materials characterisation

A Panalytical X'Pert Pro diffractometer with Ni-filtered CuKα radiation (λ = 1.5405 Å), using 40 kV and 40 m A, fitted with a X'Celerator detector was used to obtain X-ray diffraction (XRD) data at room temperature. The 2θ range 20–80° was used to record absolute scans, with a step size of 0.0167°.

A Hitachi SU6600 Scanning Electron Microscope (SEM) was used to examine the cross-sectional area of the single cell and the microstructures of the prepared catalyst.

A Stanton Redcroft STA/TGH series STA 1500 was used to perform Thermogravimetry and differential scanning calorimetry analyses. RSI Orchestrator software was used to control the Rheometric Scientific system interface used in the operation. A

N_2 atmosphere and a temperature range of room temperature to 500 °C with a heating/cooling rate of 10 °C/min and a flow rate of 50 ml/min for N_2 was used to investigate the thermal behaviour of the perovskites based cathode (LSCF).

2.3. Fabrication of the single cell for ammonia synthesis

A dry-pressing method was used to fabricate a tri-layer single cell. In order to prepared the composite anode SSCo, CGDC and a pore former (starch) were mixed in a mortar using a weight ratio of 70:30:15. CGDC/$(Li/Na/K)_2CO_3$ (70:30 wt%) were mixed to form the composite electrolyte. LSCF and CGDC and starch were mixed in a mortar to prepare the composite cathode, the same weight ratio as for the composite anode was used. The cell was prepared by feeding the composite cathode, composite electrolyte and composite anode into the die layer by layer. Uniform powder distribution was achieved with the aid of a sieve followed by uniaxially pressing at a pressure of 121 MPa to form the pellets. The as-prepared pellets were sintered for 2 h at 700 °C in air with a heating and cooling rate of 2 °C/min. An active surface area of 0.785 cm^2 was measured for the cathode. Silver paste was used as a current collector by painting it on each electrode surface of the cell in a grid pattern; Ag wires were used at both electrodes as output terminals. It has been reported that Ag is inactive for the electrochemical synthesis of ammonia [33].

2.4. Ammonia synthesis

The fabricated single cell for ammonia synthesis was mounted on a dual-chamber reactor of self design and sealed using ceramic paste (Aremco, Ceramabond 552). The following set-up was used to construct the electrolytic cell for ammonia synthesis: Air, SSCo-CGDC|CGDC-carbonate|LSCF-CGDC, 3% H_2O-N_2. Oxygen-free N_2 (BOC, purity 99.998%) was fed to the cathode after being wetted by bubbling it through room temperature water. The anode was exposed to open air. The same set-up for the dual-chamber electrochemical cell was used as reported in a previous study [34]. A Solartron 1287A/1250 electrochemical interface controlled by software CorrWare/CorrViewt for automatic data collection was used to apply a DC voltage. 20 ml of diluted HCl (0.01 M) was used to absorb the ammonia synthesised at the cathode chamber while a constant voltage was applied. This was run for 30 min. An ISE (Thermo Scientific Orion Star A214) electrode was used to analyse the concentration of NH_4^+ in the absorbed solution. The following equation was used to calculated the rate of ammonia formation:

$$r_{NH_3} = \frac{[NH_4^+] \times V}{t \times A} \quad (6)$$

Where $[NH_4^+]$ is the measured NH_4^+ ion concentration, t is the absorption time, V is the volume of the diluted HCl used for collection of ammonia, and A is the effective area of the catalyst.

A Schlumberger Solarton SI 1250 analyser was used to perform AC impedance spectroscopy (IS) measurements, coupled with a SI 1287 Electrochemical Interface controlled by Z-Plot/Z-View software. The frequency range 65 kHz–0.01 Hz was used when recording the AC impedance spectra.

3. Results and discussion

3.1. XRD analyses and SEM observation

After firing the sample at 900 °C in air for 2 h, the single phase perovskite oxide $La_{0.6}Sr_{0.4}Co_{0.2}Fe_{0.8}O_{3-\delta}$ (LSCF) was obtained (Fig. 1). The X-ray diffraction pattern of LSCF shows the typical cubic perovskite oxide structure which agrees well with the pattern from JCPDS file 89-1268 [35]. The average particle size of

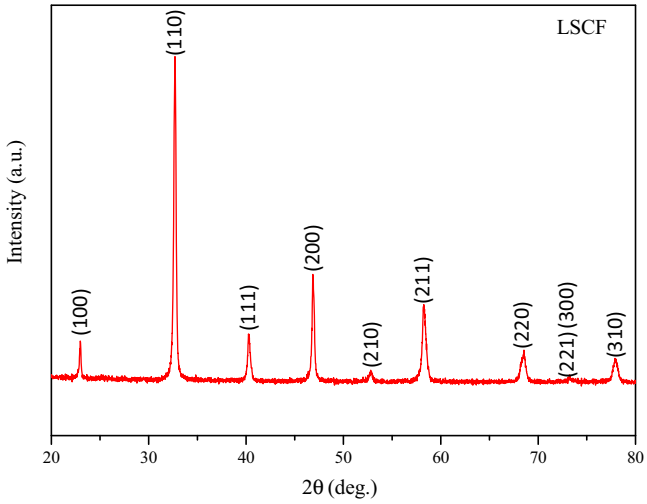

Fig. 1. XRD patterns of $La_{0.6}Sr_{0.4}Co_{0.2}Fe_{0.8}O_{3-\delta}$ (LSCF) calcined at 900 °C for 2 h.

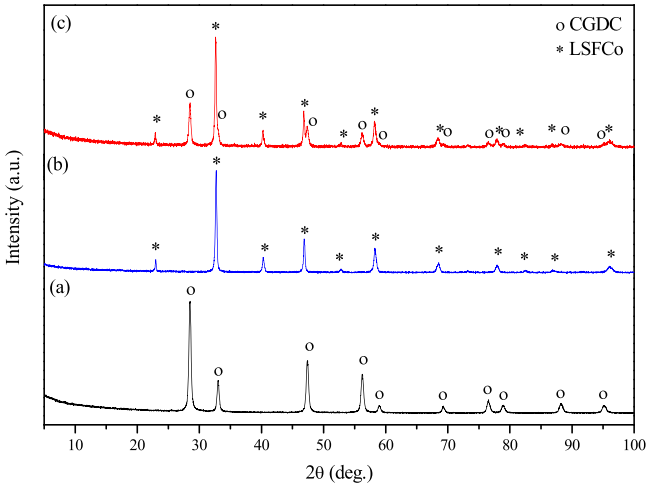

Fig. 2. XRD patterns of (a) CGDC calcined in air at 700 °C; (b) LSCF calcined in air at 900 °C; (c) LSCF-CGDC composite cathode fired in at 700 °C.

LSCF was about 31.6 nm, this estimate was calculated from Sherrer's equation. The composite cathode containing CGDC was fired at 700 °C in air for 10 h, thereby allowing the chemical compatibility between LSCF and CGDC to be investigated. The XRD patterns of CGDC, LSCF and LSCF-CGDC composite cathode (70:30 wt%) are shown in Fig. 2a–c. Only the peaks of CGDC (Fig. 2a) and LSCF (Fig. 2b) are shown in the XRD pattern of the LSCF-CGDC composite (Fig. 2c). LSCF is chemically compatible with CGDC at the cell fabricating temperature since no additional diffraction peaks were observed when the composite cathode was fired in air at 700 °C.

Scanning electron microscopy (SEM) was applied to examine the microstructure of LSCF powder calcined in air (Fig. 3a). Fine agglomerated LSCF particles with different shapes and sizes were formed. The cross sectional view shown in the SEM micrograph of the single cell (before test) sintered in air for 2 h at 700 °C is also shown in Fig. 3b. The dense CGDC-carbonate composite electrolyte can be seen, it was also shown to adhere very well to the composite cathode and anode. From this it can be indicated that there is a good thermal compatibility between the composite electrolyte and the composite electrodes.

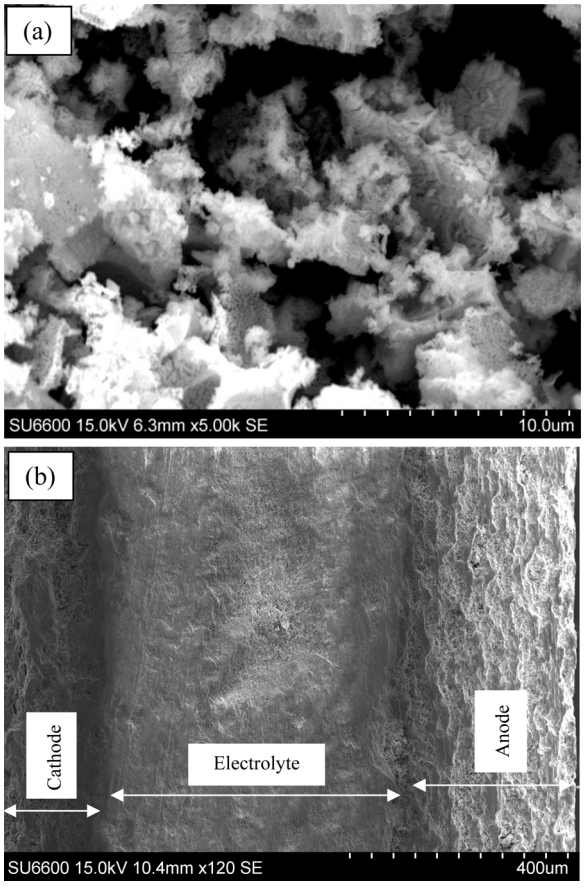

Fig. 3. SEM images; (a) LSCF calcined in air at 900 °C: (b) cross-sectional area of the single cell before test.

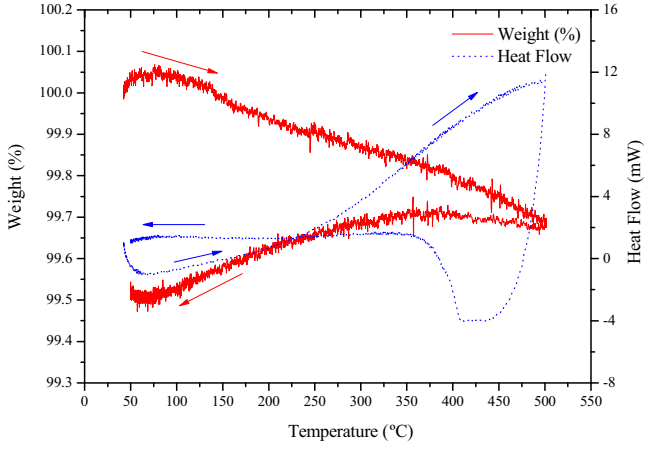

Fig. 4. TGA-DSC curves for $La_{0.6}Sr_{0.4}Co_{0.2}Fe_{0.8}O_{3-\delta}$ in nitrogen, up to 500 °C.

3.2. Thermal analysis

Due to their exposure to wet N_2 during the ammonia synthesis process, it is important to investigate its chemical compatibility of the cathode materials with N_2 at the operating temperature of the cell. The TG-DSC curve of LSCF in N_2 is shown in Fig. 4. Between room temperature and 200 °C, a small weight gain of about 0.05 wt% was observed which is possibly due to the buoyancy effect of air. The loss of lattice oxygen from $La_{0.6}Sr_{0.4}Co_{0.2}Fe_{0.8}O_{3-\delta}$, was possibly identified by the observed weight loss of 0.29 wt% between 200 and 500 °C. Most importantly, on the DSC curves no obvious thermal effects were observed therefore indicating good chemical compatibility between the LSCF cathode and N_2 within the temperature range measured.

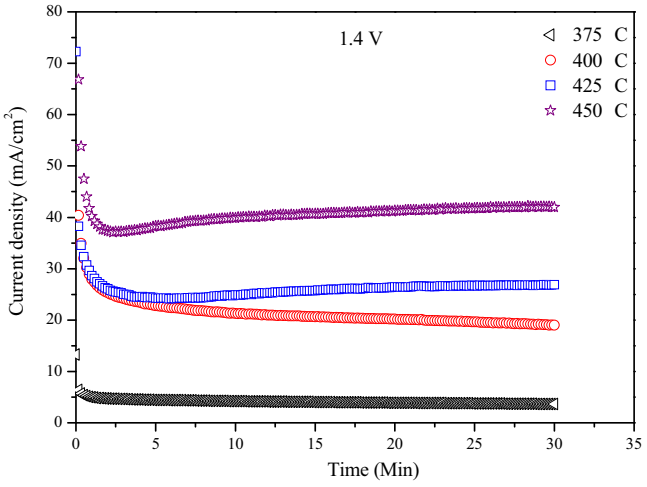

Fig. 5. Electrolytic cell performance stability at 1.4 V and 375–450 °C.

3.3. Synthesis of ammonia at different temperatures

The performance stability of the electrolytic cell based on LSCF-CGDC composite cathode over the temperature range 375–450 °C with a fixed applied voltage of 1.4 V is shown in Fig. 5. After the initial drop, the current across the cell tends to be stable at temperatures of 375 and 400 °C. The 'blocking effects' of the charged ions at the electrolyte/electrode interfaces may have been responsible for the initial current drop, this has also been observed in previous studies [12,24,36]. The current densities were shown to increase as the operating temperature was increased. The highest current density was 40.61 mA/cm^2 when the operating temperature was 450 °C, which could be attributed to the increased ionic conductivity of the electrolyte at high temperature. After the initial activation stage through applying constant voltage, the percolation pathway for ions also becomes smooth, thereby leading to higher current density. This phenomenon is very common in solid oxide fuel cells, particularly at the cathode side [30].

The in-situ AC impedance spectra recorded at different temperatures using open circuit conditions for the electrolytic cell are shown in Fig. 6a. The spectra was composed of two depressed semicircles, at high and low frequencies respectively. The impedance spectra suggest that there are at least two electrode processes, probably belonging to the cathode and anode respectively. The equivalent circuit presented in Fig. 6b was also used to fit this data. In this circuit, L is an inductance, Rs is series resistance, constant phase element is represented by CPE and R1 and R2 are polarisation resistances of the electrochemical processes. When the operating temperature of the cell was increased the series resistance Rs decreased significantly, this is shown in Fig. 6. The lowest Rs value of 3.95 Ω cm^2 was observed at 450 °C which was due to the increased ionic conductivity of the composite electrolyte at evaluated temperatures. The series resistance was significantly smaller at temperatures above 400 °C as the melting point of the mixed $(Li,Na,K)_2CO_3$ carbonates is 396 °C [37]. The melting of the carbonates resulted in an increase in ionic conductivity of the composite electrolyte thereby decreasing the series resistance. Additionally, as the operating temperature increased the total polarisation resistances, Rp (R1 + R2) also significantly decreased. This was due to the enhanced catalytic activity of the composite electrodes at evaluated

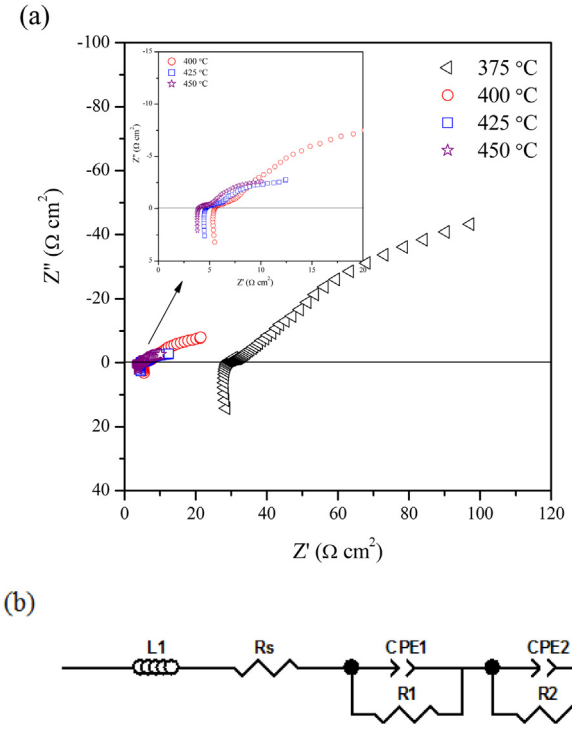

Fig. 6. (a) Impedance spectra under open circuit condition at 375–450 °C; (b) equivalent circuit for the impedance data.

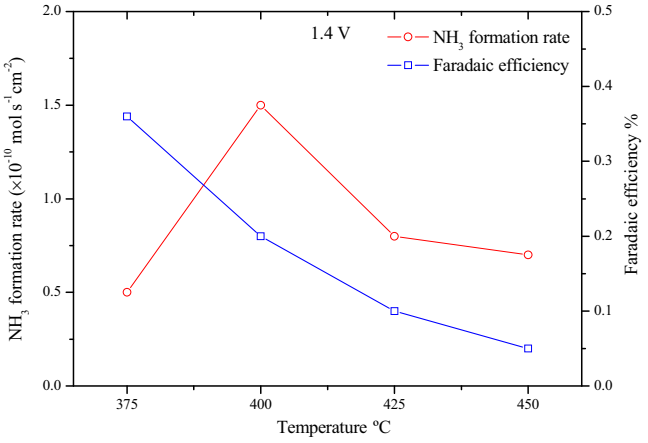

Fig. 7. Dependence of the rate of ammonia formation on the operating temperature.

temperatures. The corresponding current density was also higher as shown in Fig. 5.

The effect of operating temperature on the ammonia formation rate was also investigated under a constant voltage of 1.4 V (Fig. 7). The ammonia formation rate was shown to increase as the cell's operating temperature increased with a maximum value of 1.5×10^{-10} mol s^{-1} cm^{-2} observed when the electrolytic cell operating temperature was 400 °C. At this rate, a current density of 21.21 mA/cm^2 was observed with the corresponding Faradaic efficiency being about 0.20%. It is believed that, besides ammonia, the majority of the supplied energy was used to produce hydrogen through steam electrolysis [38]. As the operating temperature was increased past 400 °C the rate of ammonia formation started to decline. This could be attributed to the thermal decomposition of produced ammonia [39–41]. Thererfore, in order to avoid this decomposition it is desired to operate the electrochemical synthesis of ammonia at lower temepratures however, there are also other

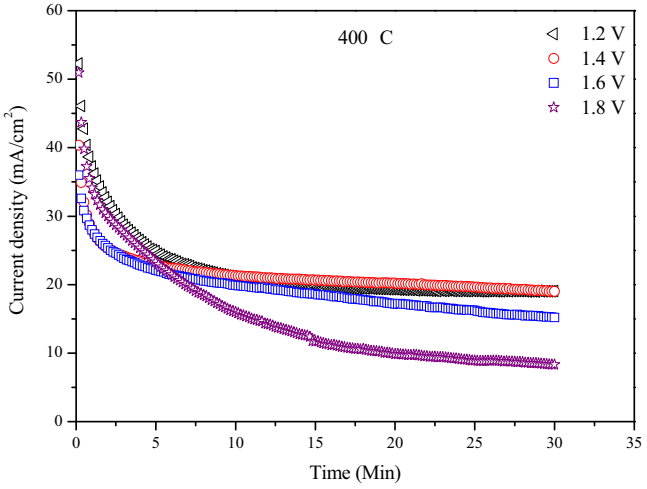

Fig. 8. Electrolytic cell performance stability at 400 °C and 1.2–1.8 V.

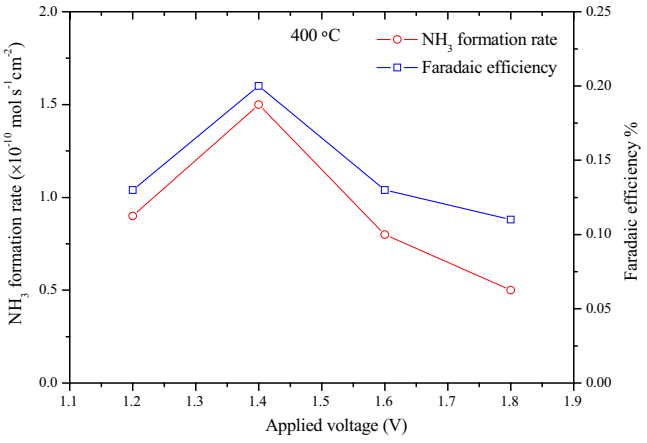

Fig. 9. Dependence of the rate of ammonia formation on the applied voltage at 400 °C.

challenges, including the low catallytic activity of the available catalysts at lower temperatures [9,42]. In the follwing study, the operating temeprature was fixed to 400 °C for ammonia synthesis.

3.4. Synthesis of ammonia at different applied voltages

The performance stability at fixed temperature (400 °C) of the cell under various applied voltages (1.2–1.8 V) is shown in Fig. 8. It was observed that at all applied voltages the current density initially decreased with this phenomenon becoming more significant at higher applied voltages. The current density was found to be up to 21.21 mA/cm^2 when the electrolytic cell was operated at 1.4 V. However, the generated current densities decreased reaching a value of 13.49 mA/cm^2 at 1.8 V. This is understandable as more charged ions will be accumulated at the electrolyte/electrode interfaces causing the blocking effect. This becomes more serious at higher voltages, partially blocking the transfer of other ions if they share the same pathway with the blocking ions [12,36]. At higher applied voltages (1.6 and 1.8 V), the current tends to decrease due to the 'blocking effect' with equilibrium not achieved during the measured period of time. This 'block effect' may be an obstacle that requires addressing in order to use the melting carbonate electrolyte in electrolytic cells for electrolyser and electrochemical synthesis.

Fig. 9 shows the ammonia formation rates under various applied voltages. Increased ammonia formation rate was observed when

the applied voltage was increased from 1.2 to 1.4 V. However, when the applied voltage was further increased to values above 1.4 V, the ammonia formation rate decreased significantly with the minimum value reached at 1.8 V. This could be attributed to the decrease in current density observed at higher applied voltages. It was therefore suspected that the cathode reaction was dominated by the competing hydrogen evolution reaction as indicated by the low ammonia formation rate, with the corresponding low Faradaic efficiencies (less than 1%) (Fig. 9). An efficient cathode catalysts for selective production of ammonia is therefore desired [38]. This led us to believe that instead of being converted to ammonia most of the transferred electrons were converted to hydrogen instead. In order to improve the Faradaic efficiency and increase the ammonia formation rate, a good catalyst which can selectively produce ammonia with poor HER activity is desired to be used as the cathode. One of the possible strategies to achieve this higher selectivity towards ammonia production is to integrate known good ammonia synthesis catalysts into the oxides, thereby forming a composite cathode increasing the selectivity to ammonia production. The observed highest ammonia formation rate (1.5×10^{-10} mol s^{-1} cm^{-2}) is about twice that of the observed ammonia formation rate (7×10^{-11} mol s^{-1} cm^{-2}) under the same experimental conditions when a Co-free cathode, $La_{0.6}Sr_{0.4}FeO_{3-\delta}$-$Ce_{0.8}Gd_{0.18}Ca_{0.02}O_{2-\delta}$ was used [24]. The possible reason for this can be attributed to the introduction of extra oxygen vacancies when some of the iron at the B-site of $La_{0.6}Sr_{0.4}FeO_{3-\delta}$ was partially replaced by cobalt as described above [28]. The increased ammonia formation activity due to the presence of oxygen vacancies in the catalysts or catalyst supporters is further confirmed by these results. Introduction of oxygen vacancies in the ammonia synthesis catalysts may improve the catalytic activity for both conventional Haber-Bosch and electrochemical synthesis processes.

4. Conclusions

A combined citrate-EDTA complexing sol-gel process was used to synthesise the $La_{0.6}Sr_{0.4}Co_{0.2}Fe_{0.8}O_{3-\delta}$ (LSCF) catalyst. X-ray diffraction (XRD) was used to characterise the catalyst along with TG-DSC analysis and scanning electron microscopy (SEM). LSCF was thermally stable in N_2 atmosphere up to 500 °C. Ammonia was successfully synthesised from wet nitrogen at atmospheric pressure using the cell made of LSCF-CGDC composite cathode, CGDC-$(Li/Na/K)_2CO_3$ composite electrolyte and SSCo-CGDC composite anode. The highest observed ammonia production rate was 1.5×10^{-10} mol s^{-1} cm^{-2} at 400 °C when the applied voltage was 1.4 V, this is higher than the observed ammonia formation rate of 7×10^{-11} mol s^{-1} cm^{-2} under the same experimental conditions when Co-free cathode, $La_{0.6}Sr_{0.4}FeO_{3-\delta}$-$Ce_{0.8}Gd_{0.18}Ca_{0.02}O_{2-\delta}$ was used as the cathode catalyst. The incorporation of steam and oxygen vacancies forming proton defect may take part in the ammonia synthesis reaction when water or steam is introduced in the system. Introduction of oxygen vacancies at the cathode is a good strategy to improve the catalytic activity for ammonia synthesis. Therefore, catalysts with high oxygen vacancies may have a higher catalytic activity for the synthesis of ammonia.

Acknowledgement

The authors gratefully thank EPSRC SuperGen XIV 'Delivery of Sustainable Hydrogen' project (Grant No EP/G01244X/1) for funding.

References

[1] M. Appl, Ammonia: Principles Industrial Practice, Wiley-VCH Weinheim, Germany, 1999.
[2] US G. Survey, Mineral Commodity Summaries, Geological Survey, 2012.
[3] R. Lan, S.W. Tao, Front. Energy Res. 2 (2014) 35.
[4] Y. Tanabe, Y. Nishibayashi, Coord. Chem. Rev. 257 (2013) 2551–2564.
[5] E. Fanone, A. Gamba, M. Prokopczuk, Energy Econ. 35 (2013) 22–34.
[6] http://www.dailymail.co.uk/news/article-2827555/Wind-farms-paid-43million-stand-idle-far-year-producing-power-National-Grid-handle.html.
[7] R. Lan, J.T.S. Irvine, S.W. Tao, Int. J. Hydrogen Energy 37 (2012) 1482–1494.
[8] G. Marnellos, M. Stoukides, Science 282 (1998) 98–100.
[9] I.A. Amar, R. Lan, C.T. Petit, S.W. Tao, J. Solid State Electrochem. 15 (2011) 1845–1860.
[10] S. Giddey, S.P.S. Badwal, A. Kulkarni, Int. J. Hydrogen Energy 38 (2013) 14576–14594.
[11] I. Garagounis, V. Kyriakou, A. Skodra, E. Vasileiou, M. Stoukides, Front. Energy Res. 2 (2014) 1.
[12] R. Lan, S.W. Tao, RSC Adv. 3 (2013) 18016–18021.
[13] S. Licht, B. Cui, B. Wang, F.-F. Li, J. Lau, S. Liu, Science 345 (2014) 637–640.
[14] E. Vasileiou, V. Kyriakou, I. Garagounis, A. Vourros, M. Stoukides, Solid State Ionics 275 (2015) 110–116.
[15] E. Vasileiou, V. Kyriakou, I. Garagounis, A. Vourros, A. Manerbino, W.G. Coors, M. Stoukides, Top. Catal. 58 (2015) 1193–1201.
[16] K. Kim, C.Y. Yoo, J.N. Kim, H.C. Yoon, J.I. Han, Korean J. Chem. Eng. 33 (2016) 1777–1780.
[17] Y. Abghoui, A.L. Garden, J.G. Howat, T. Vegge, E. Skulason, ACS Catal. 6 (2016) 635–646.
[18] K. Kim, N. Lee, C.Y. Yoo, J.N. Kim, H.C. Yoon, J.I. Han, J. Electrochem. Soc. 163 (2016) F610–F612.
[19] Y. Abghoui, A.L. Garden, V.F. Hlynsson, S. Bjorgvinsdottir, H. Olafsdottir, E. Skulason, Phys. Chem. Chem. Phys. 17 (2015) 4909–4918.
[20] http://www.hydroworld.com/articles/hr/print/volume-28/issue-7/articles/renewable-fuels-manufacturing.html;
.
[21] A. Skodra, M. Stoukides, Solid State Ionics 180 (2009) 1332–1336.
[22] I.A. Amar, C.T.G. Petit, G. Mann, R. Lan, P.J. Skabara, S.W. Tao, Int. J. Hydrogen Energy 39 (2014) 4322–4330.
[23] Y. Gong, R.L. Patel, X. Liang, D. Palacio, X. Song, J.B. Goodenough, K. Huang, Chem. Mater. 25 (2013) 4224–4231.
[24] I.A. Amar, C.T.G. Petit, R. Lan, G. Mann, S. Tao, RSC Adv. 4 (2014) 18749–18754.
[25] B. Lin, Y. Qi, K. Wei, J. Lin, RSC Adv. 4 (2014) 38093–38102.
[26] K.D. Kreuer, Chem. Mater. 8 (1996) 610–641.
[27] M. Kuhn, Y. Fukuda, S. Hashimoto, K. Sato, K. Yashiro, J. Mizusaki, J. Electrochem. Soc. 160 (2013) F34–F42.
[28] X.Y. Tan, Y.T. Liu, K. Li, Ind. Eng. Chem. Res. 44 (2005) 61–66.
[29] N.A. Baharuddin, H. Abd Rahman, A. Muchtar, A.B. Sulong, H. Abdullah, J. Zhejiang Univ. Sci. A 14 (2013) 11–24.
[30] S.P. Jiang, X. Chen, Int. J. Hydrogen Energy 39 (2014) 505–531.
[31] B. Hu, Y. Wang, C. Xia, J. Electrochem. Soc. 162 (2015) F33–F39.
[32] C.R. Xia, W. Rauch, F.L. Chen, M.L. Liu, Solid State Ionics 149 (2002) 11–19.
[33] M. Ouzounidou, A. Skodra, C. Kokkofitis, M. Stoukides, Solid State Ionics 178 (2007) 153–159.
[34] I.A. Amar, R. Lan, C.T.G. Petit, V. Arrighi, S.W. Tao, Solid State Ionics 182 (2011) 133–138.
[35] C.Y. Fu, C.L. Chang, C.S. Hsu, B.H. Hwang, Mater. Chem. Phys. 91 (2005) 28–35.
[36] L. Fan, G. Zhang, M. Chen, C. Wang, J. Di, B. Zhu, Int. J. Electrochem. Sci. 7 (2012) 8420–8435.
[37] R.I. Olivares, C. Chen, S. Wright, J. Solar Energy Eng.-Trans. Asme 134 (2012).
[38] R. Lan, K.A. Alkhazmi, I.A. Amar, S.W. Tao, Appl. Catal. B: Environ. 152–153 (2014) 212–217.
[39] I.A. Amar, C.T.G. Petit, L. Zhang, R. Lan, P.J. Skabara, S.W. Tao, Solid State Ionics 201 (2011) 94–100.
[40] W.B. Wang, X.B. Cao, W.J. Gao, F. Zhang, H.T. Wang, G.L. Ma, J. Membr. Sci. 360 (2010) 397–403.
[41] E.P. Perman, G.A.S. Atkinson, Pro. R. Soc. London 74 (1904) 110–117.
[42] R. Lan, J.T.S. Irvine, S.W. Tao, Sci. Rep. 3 (2013) 1145.